CrystEngComm

Cite this: *CrystEngComm*, 2012, **14**, 8049–8056

www.rsc.org/crystengcomm

PAPER

p-Hydroxybenzoic acid-assisted homochiral 1D-helical coordination polymers from calcium cations and cucurbit[5]uril†

Kai Chen, Li-Li Liang, Hao-Jing Liu, Zhu Tao,* Sai-Feng Xue, Yun-Qian Zhang and Qian-Jiang Zhu

Received 14th June 2012, Accepted 23rd August 2012
DOI: 10.1039/c2ce25958c

A homochiral 1D-helical coordination polymer has been assembled from calcium ions (Ca^{2+}) and cucurbit[5]uril (Q[5]) in the presence of *p*-hydroxybenzoic acid (Hyb) as an organic structure inducer. This result shows that a homochiral 1D-helical coordination polymer can be obtained from Q[5] with not only heavy lanthanides but also other metal ions, such as calcium dications in the present case, and that *p*-hydroxybenzoic acid (Hyb) can serve as an organic structure inducer in place of the previously used hydroquinone (Hyq). Control experiments by X-ray diffraction analysis have shown that Q[5] coordinates with the calcium cations to form a linear coordination polymer in the absence of Hyb, while a mixture of Q[5] and Hyb, without a metal salt under the same synthetic conditions, produces Q[5]-based linear supramolecular chains linked by hydrogen-bonding networks, which lie in a Hyb-based net.

Introduction

A supramolecular assembly generally refers to a spontaneous organization of building blocks driven by various noncovalent and coordination interactions. Among the existing assembled systems, the most cited over the last two decades are probably induced supramolecular assemblies, including surfactant-directed mesostructured materials obtained from supramolecular aggregates of long-chain alkyltrimethylammonium halides,[1] systems obtained by an induced transition from spherical to long cylindrical micelles,[2] and those obtained by the reversible preparation of stable recombinant antibodies by induced self-assembly.[3] By following the shell molt of crustaceans, Tang and co-workers recently confirmed that magnesium ions can switch off the phase transformation of hydroxyapatite, while aspartate can switch on the crystallization of hydroxyapatite (HAP, the main inorganic component of biological hard tissues such as bone and enamel).[4] It is noteworthy that the properties, structural novelties, and functionalities of the induced supramolecular assemblies can greatly exceed those obtained without using inducers or from the individual building blocks.

Cucurbit[*n*]urils (Q[*n*]s) are ideal building blocks for the construction of supramolecular assemblies because of their novel structure of a rigid hydrophobic cavity of low polarity accessible through two open polar portals rimmed with carbonyl groups.[5] The interaction of Q[*n*]s with various guest molecules has led to the proliferation of Q[*n*]-based host–guest chemistry,[6] while the interaction of Q[*n*]s with metal ions has established Q[*n*]-based coordination chemistry.[7] In Q[*n*] chemistry, it is common that the induced or triggered supramolecular assemblies are established through the Q[*n*]–guest inclusion interaction. The first induced assembly system demonstrated by Mock and co-workers involved designed substrates of alkynylammonium ions and alkyl azides undergoing an accelerated 1,3-dipolar cycloaddition reaction, yielding a substituted triazole that was included in the cavity of the cucurbituril.[8] Kim and co-workers first demonstrated a pseudorotaxane containing cucurbituril (as a molecular "bead") threaded on fluorenyltriamine (as a "string"), which behaved as a fluorescent, reversible molecular switch. The switching of the molecular bead from one site to another site on the "string", induced by a pH change, could be easily detected by changes in color and fluorescence.[9] Kim and co-workers also first demonstrated cucurbit[8]uril-induced intramolecular charge-transfer complex formation in a guest containing both an electron donor and an electron acceptor in the cucurbit[8]uril cavity.[10] Mohanty and co-workers demonstrated salt-induced guest relocation from a macrocyclic cavity of cucurbit[7]uril into a biomolecular pocket of bovine serum albumin.[11] Brunsveld and co-workers demonstrated protein dimerization induced by supramolecular interactions with cucurbit[8]uril.[12] These research results could hold promise for potential applications in catalysis, molecular machines, materials, polymers, and biochemistry.

Compared to Q[*n*]-based host–guest chemistry, few examples of supramolecular self-assemblies induced by organic molecules have been reported in Q[*n*]-based coordination chemistry. Although Buschmann and co-workers extensively studied Q[6]

Key Laboratory of Macrocyclic and Supramolecular Chemistry of Guizhou Province, Guizhou University, Guiyang 550025, People's Republic of China. E-mail: kaichen85@gmail.com (K.C.); gzutao@263.net (Z.T.); Fax: +86-851-3620906 (Z. T.); Tel: +86-851-3620906 (Z. T.)

† Electronic supplementary information (ESI) available: PXRD patterns, ^{1}HNMR, TG curves, DSC curves and X-ray crystallographic information. CCDC reference numbers 882714–882716 and 895165. For ESI and crystallographic data in CIF or other electronic format see DOI: 10.1039/c2ce25958c

systems incorporating organic dyes and heavy metal ions during the early stages of Q[*n*] chemistry, their works were focused on the interaction of cucurbituril with the dyes or the heavy metal ions, respectively.[13] In their Q[6]–metal ion–organic molecule ternary system, Kim and co-workers developed a strategy that involved threading cucurbituril (Q[6]) molecules with a long chain with two active ends, and then allowing the resulting pseudorotaxane to coordinate with metal ions; coordination took place between the metal ions and the long-chain guests, but also with Q[6] in the resulting novel Q[6]-based supramolecular architectures.[14] Fedin and co-workers selected cucurbituril as the supporting ligand for the isolation of tetranuclear lanthanide complexes from aqueous solution.[15] Following on from Fedin's work, Thuéry has demonstrated a series of novel uranyl–Q[*n*] and lanthanide–Q[*n*] supramolecular assemblies in the presence of additional organic molecules.[16] Since we identified a stable Q[5]-based MOF structure made up of "beaded" rings, built with the assistance of a *p*-hydroxybenzoic acid structure inducer,[17] the coordination of metal ions to Q[*n*]s in the presence of organic molecules or an inorganic species has been extensively studied in our laboratory, and a strategy of third species-induced direct coordination of metal ions to Q[*n*]s has been gradually established. We recently reported a series of one-dimensional polymers,[18] two-dimensional networks,[18*a*] and three-dimensional frameworks[19] by using this strategy. More recently, we synthesized and characterized homochiral 1D-helical coordination polymers from achiral cucurbit[5]uril and heavy lanthanides by hydroquinone (Hyq)-induced spontaneous resolution;[20,21] however, under the same synthetic conditions, the coordination of lighter lanthanides to cucurbit[5]uril gave linear molecular chains or molecular pairs, which were completely different from those with the heavy lanthanides.[21] These results suggested that the supramolecular self-assemblies could be dramatically affected by subtle differences in the properties of the components.

Herein, we report our recent success in preparing another homochiral 1D-helical coordination polymer of cucurbit[5]uril with calcium dications, induced by *p*-hydroxybenzoic acid (Hyb). Compared to the Q[5]–Ln^{3+}–Hyq systems,[20] both the metal ion and organic structure inducer are different in the system in the present work, suggesting that the formation of homochiral 1D-helical coordination polymers or other novel supramolecular self-assemblies could be an intrinsic property of Q[5] that is manifested under appropriate synthetic conditions, in the presence of suitable organic inducers and metal ions.

Experimental section

General materials

Chemicals, such as calcium chloride, *p*-hydroxybenzoic acid and hydrochloride acid, were of reagent grade and were used without further purification. Q[5] was prepared as reported elsewhere.[5*b*,*c*] Elemental analyses were carried out on a EURO EA-3000 elemental analyzer.

Preparation of {$Ca_2(H_2O)$ Cl@Q[5]}·3Cl·12(H_2O) (1)

A mixture of Q[5]·10H_2O (50 mg, 0.05 mmol) and $CaCl_2$ (33.3 mg, 0.30 mmol) in ~5 mL of 1.0 mol L^{-1} HCl was refluxed for 5 min and then filtered. Leaving the filtrate to stand yielded colorless crystals of complex **1** within 2 days (26% yield based on Q[5]·10H_2O). Elemental analysis calcd. (%) for $C_{30}H_{56}N_{20}O_{23}Ca_2Cl_4$: C 28.00, H 4.39, N 21.77; found: C 28.47, H 4.22, N 21.94.

Preparation of Q[5]·2Hyb·13H_2O (2)

A mixture of Q[5]·10H_2O (50 mg, 0.05 mmol) and Hyb (25.2 mg, 0.20 mmol) in ~5 mL of 1.0 mol L^{-1} HCl was refluxed for 5 min and then filtered. Leaving the filtrate to stand yielded colorless crystals of complex **2** within 7 days (42% yield basis on Q[5]·10H_2O). Elemental analysis calcd. (%) for $C_{44}H_{68}N_{20}O_{29}$: C 39.41, H 5.11, N 20.89; found: C 39.77, H 4.92, N 21.24.

Preparation of {$Ca(H_2O)_4$Q[5]}·Hyb·2Cl·12H_2O (3)

Q[5]·10H_2O (50 mg, 0.05 mmol) and a fourfold excess of Hyq (25.2 mg, 0.20 mmol) were dissolved in ~5 mL of 1.0 mol L^{-1} HCl at 50 °C and the mixture was stirred until the Q[5] and Hyq had completely dissolved. A sixfold excess of $CaCl_2$ (33.3 mg, 0.30 mmol) was then added with stirring. The solution was left to stand, allowing slow evaporation of the volatiles in air at room temperature. Colorless crystals were obtained from the solution over the course of 14 days. The yield, based on cucurbit[5]uril, was 56%. Elemental analysis calcd. (%) for $C_{37}H_{68}N_{20}O_{29}CaCl_2$ (%): C 32.48, H 5.01, N 20.48; found: C 32.88, H 4.91, N 20.36.

X-Ray crystallography

A suitable single crystal (~0.2 × 0.2 × 0.1 mm^3) was taken up in paraffin oil and mounted on a Bruker SMART Apex II CCD diffractometer equipped with a graphite-monochromated Mo-Kα (λ = 0.71073 Å, μ = 0.828 mm^{-1}) radiation source operating in the ω-scan mode and a nitrogen cold stream (−50 °C). Data were corrected for Lorentz and polarization effects (SAINT),[22] and semi-empirical absorption corrections based on equivalent reflections were also applied (SADABS).[22] The structure was elucidated by direct methods and refined by the full-matrix least-squares method on F2 with the SHELXS-97 and SHELXL-97 program packages, respectively.[23] All non-hydrogen atoms were refined anisotropically. Carbon-bound hydrogen atoms were introduced at calculated positions, and were treated as riding atoms with an isotropic displacement parameter equal to 1.2 times that of the parent atom. Most of the water molecules in the compounds were omitted using the SQUEEZE option of the PLATON program. Analytical expressions for neutral-atom scattering factors were employed, and anomalous dispersion corrections were incorporated. Details of the crystal parameters, data collection conditions, and refinement parameters for compounds **1–3** are summarized in Table 1. The *R* factors of compound **1** are a bit high because the crystal of compound **1** is easy weathered, even in low temperatures. In the crystal structure of compound **3**, we have tried to model the atoms (Hyb) with large ADPs as disordered, but this did not give a better solution, and to better understand the structure of compound **3**, the ^{1}H-NMR results confirmed the Hyb and Q[5] ratio of 1 : 1. In addition, the crystallographic data for the reported structures has been provided (CCDC numbers 882714 (**1**), 882715 (**2**) and 882716 (**3**).†

Table 1 Crystal data and structure refinement details for compounds **1–3**

Compound	**1**	**2**	**3**
Empirical formula	$C_{30}H_{56}N_{20}O_{23}Ca_2Cl_4$	$C_{44}H_{68}N_{20}O_{29}$	$C_{37}H_{68}N_{20}O_{29}CaCl_2$
Formula weight	1286.91	1341.18	1368.09
Crystal system	Monoclinic	Orthorhombic	Hexagonal
Space group	*C* 2/*c*	*P* 21 21 2	*P* 65
a/Å	32.7209(15)	15.8841(18)	14.7327(18)
b/Å	19.4444(9)	12.4803(14)	14.7327(18)
c/Å	32.739(2)	14.1747(16)	46.389(11)
β/°	115.904(2)	90.00	90.00
V/Å^3	18737.2(18)	2810.0(5)	8720(3)
Z	16	2	6
D_c/g cm^{-3}	1.515	1.585	1.563
T/K	173	223	173
μ/mm^{-1}	0.547	0.134	0.306
Unique reflect.	16 474	4965	10 098
Obs. reflect.	5345	4628	8730
R_{int}	0.0802	0.0233	0.0485
R_1 [$I > 2\sigma(I)$][a]	0.1015	0.0466	0.0762
wR_2 [$I > 2\sigma(I)$][b]	0.2565	0.1282	0.2124
R (all data)	0.1753	0.0496	0.0825
wR (all data)	0.2591	0.1303	0.2189
GOF on F^2	1.097	1.080	1.032

[a] $R_1 = \sum||F_o| - |F_c||/\sum|F_o|$. [b] $wR_2 = |\sum w(|F_o|^2 - |F_c|^2)|/\sum|w(F_o)^2|^{1/2}$, where $w = 1/[\sigma^2(F_o^2) + (aP)^2 + bP]$; $P = (F_o^2 + 2F_c^2)/3$.

Results and discussion

In order to better understand the influences of the organic structure inducer on the construction of the homochiral 1D-helical coordination polymers, the coordination of Q[5] with calcium dications, and the interaction of Q[5] with the organic structure inducer Hyb in the solid state were also investigated following preparations under similar synthetic conditions. The reaction of Q[5] with calcium chloride in 1.0 mol L^{-1} aqueous HCl solution resulted in colorless crystals of the compound $\{[Ca_2(H_2O)Cl@Q[5]]\}\cdot 3Cl\cdot 12H_2O$ (**1**). The single-crystal X-ray structure of compound **1** shows that linear coordination polymers are constructed from Q[5]–Ca^{2+} molecular capsules linked by coordination of the coordinated Ca^{2+} to a portal carbonyl oxygen of the neighboring Q[5]–Ca^{2+} molecular capsule, as shown in Fig. 1a. The asymmetric unit of compound **1** consists of two Q[5] molecules, four Ca^{2+} cations, eight chloride anions, and two coordinated water molecules. A view of the Q[5]–Ca^{2+} molecular capsules is shown in Fig. 1b; each Ca^{2+} ion coordinates to six oxygen atoms, that is, five portal carbonyl oxygen atoms of Q[5] in the molecular capsule, plus a coordinated water molecule O1W or O2W for Ca1 or Ca3,

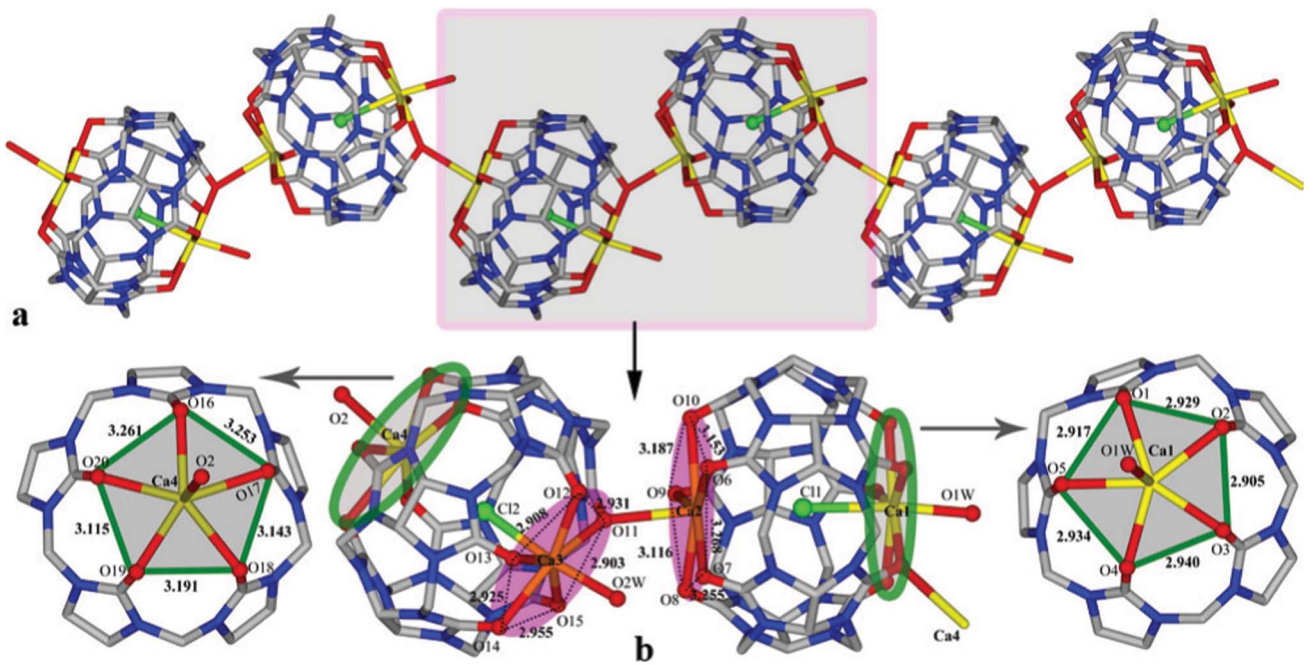

Fig. 1 (a) A linear supramolecular chain constructed from Q[5]–Ca^{2+} molecular capsules linked by additional Ca–$O_{carbonyl}$ bonds; (b) view of the Q[5]–Ca^{2+} molecular capsules.

respectively; O11 or O2 for Ca2 or Ca4, respectively, with the latter also coordinating to a coordinated chloride anion Cl1 or Cl2 included in the cavity of the Q[5]. Close inspection reveals that the sizes of the two portals of the capsules are different; the portal lidded with Ca2 or Ca4 is larger than that lidded with Ca1 or Ca2 (see Fig. 1b). The Ca1 or Ca3–$O_{carbonyl}$ bond lengths are in the range 2.431–2.535 Å, while the Ca2 or Ca4–$O_{carbonyl}$ bond lengths are in the range 2.686–2.751 Å. Moreover, the Ca2–O11

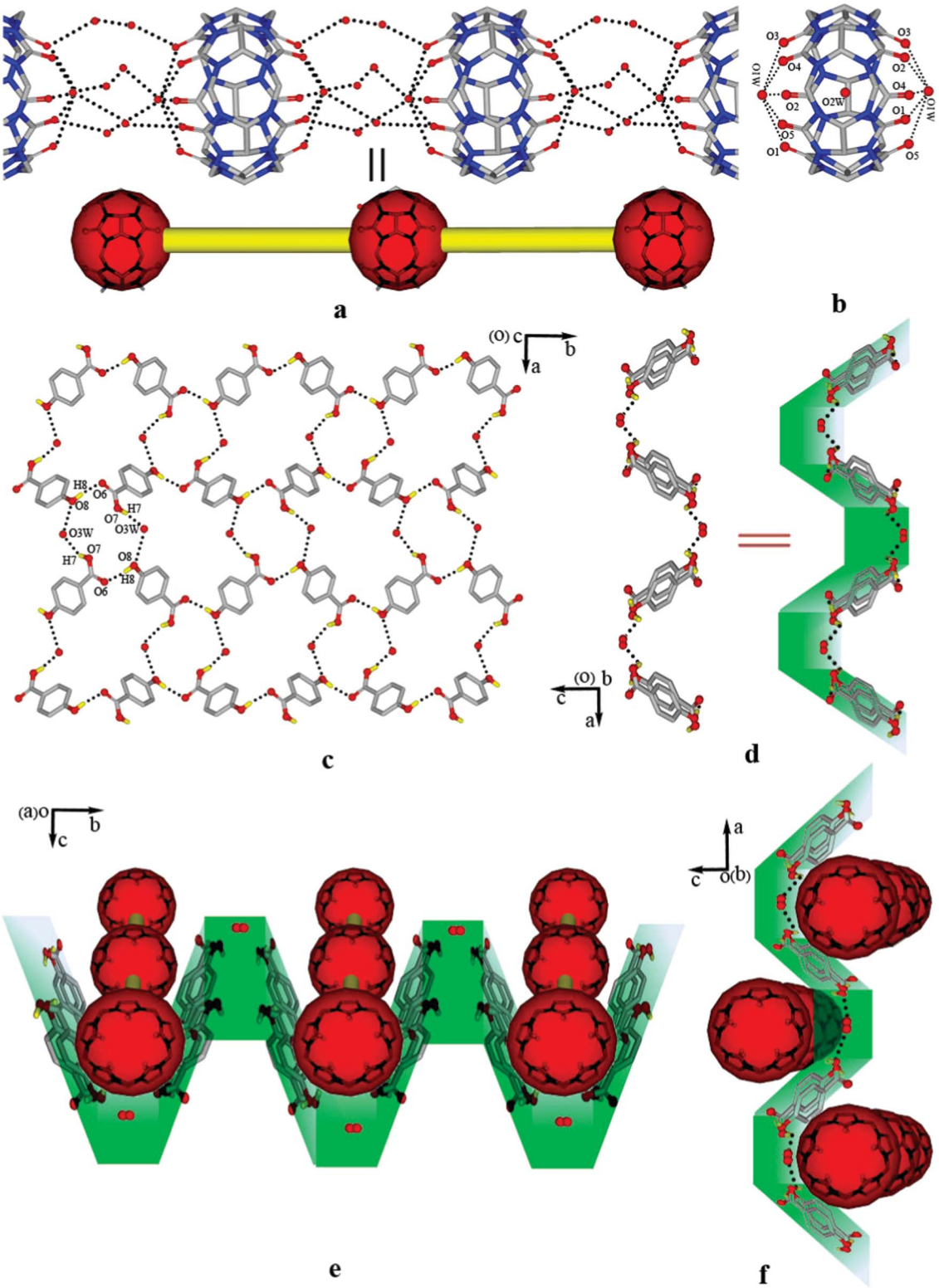

Fig. 2 (a, b) A linear supramolecular chain constructed of H_2O–H_2O@Q[5]–H_2O molecular capsules linked by hydrogen-bonding networks extending along the *b*-axis; (c–d) views of the Hyb molecular net; (e) and (f) views of the Hyb molecular net overlaid with the Q[5]-based molecular chain.

(2.843 Å) and Ca4–O2 (2.840 Å) bond lengths are much longer than those in the capsules.

Similar linear coordination polymers can be observed in the crystal structure of the complex of Q[5]–K^+;[24] however, the sizes of the two lidded portals of the Q[5]–K capsules are almost the same, the K–$O_{carbonyl}$ bond lengths are in the ranges 2.650–2.776 Å and 2.717–2.769 Å, respectively, and the bond length of the K^+ lid to the additional carbonyl oxygen of the neighboring Q[5] (2.741 Å) is shorter than that in the present case (see SI-Fig. 1 in the ESI†). Comparison of the ionic radii of potassium and calcium shows that the former (1.33 Å) is 0.34 Å larger than the latter (0.99 Å); if the normal K–$O_{carbonyl}$ bond length is about 2.7 Å, the normal Ca–$O_{carbonyl}$ bond length should be in the range 2.4–2.5 Å. It is unusual that the Ca–$O_{carbonyl}$ bond lengths are longer than 2.6 Å, even up to 2.8 Å in the present case.

A mixture of Q[5] and Hyb without any metal salt in 1.0 mol L^{-1} HCl aqueous solution yielded colorless crystals of compound Q[5]·2Hyb·13H_2O (**2**). The single-crystal X-ray structure of compound **2** showed that linear supramolecular chains, extending along the *b*-axis, were constructed from H_2O–H_2O@Q[5]–H_2O molecular capsules linked by complicated hydrogen-bonding networks, as shown in Fig. 2a. The H_2O–H_2O@Q[5]–H_2O molecular capsule in the chain, as depicted in Fig. 2b, shows that two water molecules O1W cover the respective portals of the Q[5] molecule through hydrogen bonding, and a water molecule O2W is included in the cavity of the Q[5] molecule. The O1W–$O_{carbonyl}$ distances are in the range 2.779–3.010 Å. It is notable that the Hyb molecules "knit" a large molecular net with a wave-like shape in the *ab* plane through hydrogen bonding (see Fig. 2c–d). The O8–H8···O6 hydrogen bonds lead to the formation of a Hyb molecular chain in a head-to-tail manner; the O7–H7···O3W hydrogen-bonding interaction and the O3W···O8 interaction link the Hyb chains in the net. The Q[5]-based molecular chains lie in the troughs of the Hyb net (see Fig. 2e and f). The question then arose as to the nature of the driving forces responsible for the formation of such Q[5]-Hyb supramolecular assemblies. Close inspection reveals that four Hyb molecules are close to each Q[5] molecule in the supramolecular assembly, and that the aromatic ring of each Hyb molecule is almost parallel to the five-membered rings of the glycouril moieties of the neighboring Q[5] molecules; the distances between the two planes are in the range 3.497–3.561 Å (see Fig. 3a and b). Various kinds of interactions could be involved in such a supramolecular assembly, but the most common of these should be the π···π interaction between the phenyl ring of Hyb and the portal carbonyl group of Q[5]; the distances between the two π-bonds are 2.973–2.465 Å.[20] A secondary interaction could be the C–H···π interaction between the phenyl ring of Hyb and the methine groups of Q[5]; the distances between the methine proton and the phenyl ring are 3.497–3.561 Å (Fig. 3a and b).[20,21,25,26] Chen and Yamauchi first proposed exploration of the chemical behavior of the convex-shaped outer walls, and found that the convex-shaped glycoluril backbones of Q[6] displayed a much higher affinity for aromatic rings than other Q[6]′ units.[27] This is borne out in the present case, and in compound **2** it could be ascribed to π···π and C–H···π interactions.

In the presence of the organic molecule Hyb, reaction of Q[5] with calcium chloride resulted in colorless crystals of the compound {$Ca(H_2O)_4$Q[5]}·Hyb·2Cl·12H_2O (**3**). Single-crystal X-ray diffraction analyses revealed that **3** crystallized in the space group $P6_5$ and it was very similar to the compounds obtained from reactions of Q[5] with the nitrates of heavy lanthanides, such as Dy^{3+}, Er^{3+}, Yb^{3+}, or Lu^{3+}, in the presence of the organic molecule hydroquinone (Hyq). Single-crystal X-ray diffraction analyses revealed that the two enantiomers crystallized in the Sohncke space groups $P6_1$ and $P6_5$. Coordination of Dy^{3+} to the portal carbonyl resulted in the formation of a Q[5]-based helical polymer; in particular, the Q[5]-based helical polymers, with the space group $P6_1$are all right-handed helices, while those with space group $P6_5$ are all left-handed helices. Moreover, every crystal in a single cluster of crystals is of the same space group and displays the same absolute structure, suggesting chiral symmetry breaking.[20,21] In the present work, the crystal structure of compound **3** also shows a Q[5]-based helical polymer and every crystal is of the same space group and displays the same absolute structure (see Fig. 4a and b). In compound **3**, each Ca^{2+} ion is eight-coordinated by four water molecules and four carbonyl groups from two neighboring Q[5] molecules. It is notable that the Ca–$O_{carbonyl}$ bond lengths are much shorter than those observed in compound **1**; they are in the range 2.389–2.450 Å (see Fig. 4c). The coordination of alternating Ca^{2+} ions and Q[5] molecules leads to the formation of a one-dimensional polymer, specifically a left-handed helical coordination polymer. In ref. 20, the coordinated Q[5] was regarded as a bidentate ligand to one Dy^{3+} ion center; each Dy^{3+} ion was coordinated by two bidentate ligands with the same Δ/Λ chirality, and it may be for this reason that the chain was twisted and a homochiral right- or left-handed helical structure was ultimately formed.

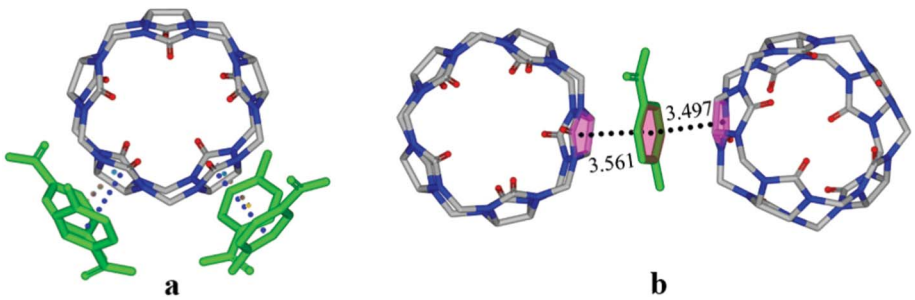

Fig. 3 (a) Arrangement of each Q[5] molecule with neighboring Hyb molecules, and (b) arrangement of each Hyb molecule with neighboring Q[5] molecules in the supramolecular assembly.

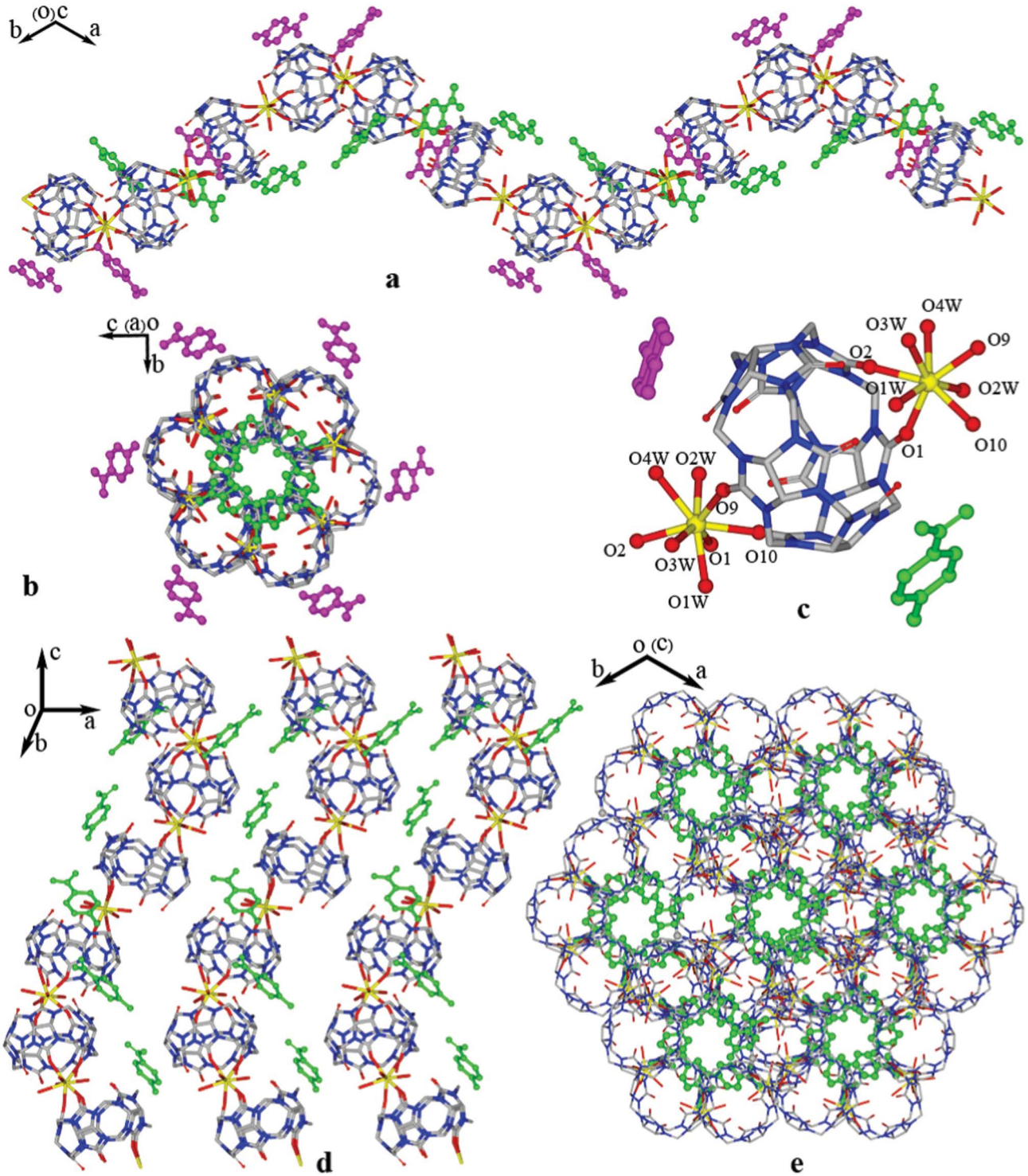

Fig. 4 X-Ray structures of the chiral helical Q[5]–Ca^{2+} coordination polymer extending along the *c*-axis accompanied by Hyb-based left-handed helices, (a) side view and (b) top view, (c) the basic interaction between Q[5], Ca^{2+}, and Hyb; stacking of the helical polymers (d) side view and (e) top view. Hydrogen atoms have been omitted for clarity.

On the other hand, the interactions of Hyb molecules with Q[5] molecules could be a more important driving force leading to the formation of Q[5]-based helical polymers, in which the Hyb molecules encircle the helical polymer and form a Hyb-based left-handed helix. Each Q[5]-based helical polymer is accompanied by two Hyb-based left-handed helices, one (shown in white) is fixed inside the channel of the Q[5]-based helical polymer, while the other (shown in green) is fixed outside the channel of the Q[5]-based helical polymer (Fig. 4a and b). Close inspection reveals that each aromatic plane of Hyb in the Hyb-based helix is almost parallel to one of the five-membered rings of glycouril in the Q[5] molecule as a result of π···π stacking of

the phenyl ring of Hyb and the carbonyl group of Q[5], as well as C–H···π interactions between the phenyl ring of Hyb and the methine groups of Q[5] (see Fig. 4c). In compound **2**, it can be seen that each Q[5] molecule is supported by four Hyb molecules, with a symmetrical arrangement induced by π···π stacking interactions (see Fig. 3a), which leads to the formation of linear Q[5]-based chains through hydrogen bonding (see Fig. 2a). In compound **3**, however, each Q[5] molecule is accompanied by two Hyb molecules in an unsymmetrical arrangement (see Fig. 4c). Thus, the combination of the Λ-chiral Ca^{2+}–Q[5] complexes and two unsymmetrically arranged Hyb molecules results in the formation of a Q[5]-based left-handed helical polymer accompanied by two Hyb-based helices. Moreover, each Q[5]-based helical polymer is surrounded by six neighbors, as shown in Fig. 4d and e. It is believed that this arrangement may be stabilized by the π···π stacking interactions between the phenyl ring of Hyq and the carbonyl group of Q[5], as well as the C–H···π interactions between the phenyl ring of Hyq and the methine groups of Q[5].

Characterization of related compounds

The crystal structure of compound **3** shows three components: Q[5], a Ca dication, and the structure inducer Hyb in a 1 : 1 : 1 ratio. This is further confirmed by the ^{1}H NMR results. The integrals of the doublets due to the phenyl protons (at δ = 7.8 and 6.8) relative to those of the three different Q[5] protons indicate a macrocyclic ligand to Hyb ratio of 1 : 1 (see SI-Fig. 2 in the ESI†).

The powder patterns of compounds **1** and **3** show obvious crystalline phases of the compounds before they are destroyed by heating. Comparison of the powder X-ray diffraction (PXRD) patterns of compounds **1** and **3** with the corresponding simulations shows that the samples produced were pure phases (see SI-Fig. 3 in the ESI†).

Thermal analysis reveals that the DSC and TG curves of compounds **1** and **3** are essentially consistent with their crystal structures (see SI-Fig. 4 in the ESI†). Comparison of the DSC and TG curves indicates that compound **1** has two endothermic bands in the range from room temperature to 200 °C, with a weight loss of ~16%, corresponding to the unbound and bound water molecules (the expected weight loss of water molecules in compound **1** is ~15%), and the decomposition temperature of Q[5] in compound **1** is ~528 °C. Similarly, comparison of the DSC and TG curves of compound **3** shows an endothermic band in the range from room temperature to 200 °C with a weight loss of ~16% corresponding to the uncoordinated water molecules (the expected weight loss of water molecules in compound **3** is indeed ~16%); the endothermic band with a weight loss of 8.5% corresponds to the sublimation of Hyb molecules (the expected weight loss of Hyb in compound **3** is ~9%); the decomposition temperature of Q[5] in compound **3** is ~514.7 °C.

Conclusion

In the present work, we have demonstrated a Q[5]-based homochiral 1D-helical coordination polymer. Compared to the previously reported Q[5]–Ln^{3+}–Hyq homochiral 1D-helical coordination polymers, both the metal ion and the organic structure inducer are different; that is, they are Ca^{2+} as the metal ion and *p*-hydroxybenzoic acid (Hyb) as the organic species. The findings suggest that the formation of a homochiral 1D-helical coordination polymer[20,21] or other novel supramolecular self-assemblies[17,18a,b] could be an intrinsic property of Q[5] that is manifested under appropriate synthetic conditions, in the presence of appropriate organic inducers and metal ions. Our results have proved that the coordination of Ca^{2+} cations to Q[5] can lead to the formation of linear one-dimensional polymers, and that the presence of small aromatic compounds, such as hydroquinone, or *p*-hydroxybenzoic acid as used in the present work, can regulate the arrangement of the macrocyclic ligand Q[5] through π···π stacking of the phenyl ring of Hyb and the carbonyl group of Q[5], as well as C–H···π interactions between the phenyl ring of Hyb and the methine groups of Q[5]. Specifically, the combination of Ca^{2+} and Hyb with Q[5] results in the formation of Q[5]–Ca^{2+}–Hyb homochiral 1D-helical coordination polymers. Further detailed investigations towards a better understanding of this chemistry are ongoing in our laboratories.

Acknowledgements

This work was supported by the National Natural Science Foundation of China (no. 20961002; 21101037); the Natural Science Foundation of the Department of Education of Guizhou Province, the Science and Technology Fund of Guizhou Province, the International Collaborative Project Fund of Guizhou Province, and the "Chun-Hui" Funds of the Chinese Ministry of Education are also gratefully acknowledged.

References

1 (*a*) Y. Lu, *Angew. Chem., Int. Ed.*, 2006, **45**, 7664; (*b*) F. Hoffmann, M. Cornelius, J. Morell and M. Froba, *Angew. Chem., Int. Ed.*, 2006, **45**, 3216.
2 C. A. Dreiss, *Soft Matter*, 2007, **3**, 956.
3 C. Sanchez, H. Arribart and M. M. G. Guille, *Nat. Mater.*, 2005, **4**, 277.
4 (*a*) J. H. Tao, D. M. Zhou, Z. S. Zhang, X. R. Xu and R. K. Tang, *Proc. Natl. Acad. Sci. U. S. A.*, 2009, **106**, 22096; (*b*) X. Chu, W. Jiang, Z. Zhang, Y. Yan, H. Pan, X. Xu and R. K. Tang, *J. Phys. Chem. B*, 2011, **115**, 1151.
5 (*a*) W. A. Freeman, W. L. Mock and N. Y. Shih, *J. Am. Chem. Soc.*, 1981, **103**, 7367; (*b*) A. I. Day and A. P. Arnold, Method for synthesis cucurbiturils, *WO* 0068232, 2000, **8**; (*c*) J. Kim, I. S. Jung, S. Y. Kim, E. Lee, J. K. Kang, S. Sakamoto, K. Yamaguchi and K. Kim, *J. Am. Chem. Soc.*, 2000, **122**, 540; (*d*) A. I. Day, R. J. Blanch, A. P. Arnold, S. Lorenzo, G. R. Lewis and I. Dance, *Angew. Chem., Int. Ed.*, 2002, **41**, 275.
6 Reviews: (*a*) J. Jason Lagona, P. Mukhopadhyay, S. Chakrabarti and L. Isaacs, *Angew. Chem., Int. Ed.*, 2005, **44**, 4844; (*b*) Y. H. Ko, E. Kim, I. Hwang and K. Kim, *Chem. Commun.*, 2007, 1305; (*c*) V. Sindelar, S. Silvi, S. E. Parker, D. Sobransingh and A. E. Kaifer, *Adv. Funct. Mater.*, 2007, **17**, 694; (*d*) N. J. Wheate, *J. Inorg. Biochem.*, 2008, **102**, 2060; (*e*) L. Isaacs, *Chem. Commun.*, 2009, 619; (*f*) W. Wang and A. E. Kaifer, *Adv. Polym. Sci.*, 2009, **222**, 205; (*g*) S. Gadde and A. E. Kaifer, *Curr. Org. Chem.*, 2011, **15**, 27; (*h*) E. Masson, X.-X. Ling, R. Joseph, L. Kyeremeh-Mensah and X.-Y. Lu, *RSC Adv.*, 2012, **2**, 1213.
7 Reviews: (*a*) O. A. Gerasko, M. N. Sokolov and V. P. Fedin, *Pure Appl. Chem.*, 2004, **76**, 1633; (*b*) H. Cong, Q. J. Zhu, S. F. Xue, Z. Tao and G. Wei, *Chin. Sci. Bull.*, 2010, **55**, 3633.
8 W. L. Mock, T. A. Irra, J. P. Wepsiec and T. L. Manimaran, *J. Org. Chem.*, 1983, **48**, 3619.
9 S. I. Jun, J. W. Lee, S. Sakamoto, K. Yamaguchi and K. Kim, *Tetrahedron Lett.*, 2000, **41**, 471.

10 J. W. Lee, K. Kim, S. W. Choi, Y. H. Ko, S. Sakamoto, K. Yamaguchi and K. Kim, *Chem. Commun.*, 2002, 2692.
11 M. Shaikh, J. Mohanty, A. C. Bhasikuttan, V. D. Uzunova and W. M. Nau, *Pal, H. : Chem. Commun.*, 2008, 3681.
12 H. D. Nguyen, D. T. Dang, J. L. J. van Dongen and L. Brunsveld, *Angew. Chem., Int. Ed.*, 2010, **49**, 895.
13 (*a*) H. J. Buschmann and E. Schollmeyer, *Textilveredlung*, 1998, **33**, 44; (*b*) R. Hoffmann, W. Knoche, C. Fenn and H. J. Buschmann, *J. Chem. Soc., Faraday Trans.*, 1994, **90**, 1507.
14 (*a*) D. Whang, Y. M. Jeon, J. Heo and K. Kim, *J. Am. Chem. Soc.*, 1996, **118**, 11333; (*b*) K. M. Park, J. Heo, S. G. Roh, Y. M. Jeon, D. Whang and K. Kim, *Mol. Cryst. Liq. Cryst. Sci. Technol., Sect. A*, 1999, **327**, 65; (*c*) J. Heo, S. Y. Kim, S. G. Roh, K. M. Park, G. J. Park, D. Whang and K. Kim, *Mol. Cryst. Liq. Cryst. Sci. Technol., Sect. A*, 2000, **342**, 29.
15 (*a*) O. A. Geraśko, E. A. Mainicheva, M. I. Naumova, M. Neumaier, M. M. Kappes, S. Lebedkin, D. Fenske and V. P. Fedin, *Inorg. Chem.*, 2008, **47**, 8869; (*b*) O. A. Geraśko, E. A. Mainicheva, M. I. Naumova, O. P. Yurjeva, A. Alberola, C. Vicent, R. Llusar and V. P. Fedin, *Eur. J. Inorg. Chem.*, 2008, 416.
16 (*a*) P. Thuéry, *Inorg. Chem.*, 2010, **49**, 9078; (*b*) P. Thuéry and B. Masci, *Cryst. Growth Des.*, 2010, **10**, 716; (*c*) P. Thuéry, *Cryst. Growth Des.*, 2011, **11**, 2606; (*d*) P. Thuéry, *Inorg. Chem.*, 2011, **50**, 10558.
17 X. Feng, K. Chen, Y.-Q. Zhang, S.-F. Xue, Q.-J. Zhu, Z. Tao and A. I. Day, *CrystEngComm*, 2011, **13**, 5049.
18 (*a*) K. Chen, L.-L. Liang, Y.-Q. Zhang, Q.-J. Zhu, S.-F. Xue and Z. Tao, *Inorg. Chem.*, 2011, **50**, 7754; (*b*) K. Chen, X. Feng, L.-L. Liang, Y.-Q. Zhang, Q.-J. Zhu, S.-F. Xue and Z. Tao, *Cryst. Growth Des.*, 2011, **11**, 5712; (*c*) W.-J. Chen, D.-H. Yu, Y.-Q. Zhang, Q.-J. Zhu, S.-F. Xue, Z. Tao and G. Wei, *Inorg. Chem.*, 2011, **50**, 6956; (*d*) X. Feng, H. Du, K. Chen, X. Xiao, S.-X. Luo, S.-X. Xue, Y.-Q. Zhang, Q.-J. Zhu, Z. Tao, X.-Y. Zhang and W. Gang, *Cryst. Growth Des.*, 2010, **10**, 2901.
19 K. Chen, H. Cong, X. Xiao, Y.-Q. Zhang, S.-F. Xue, Z. Tao, Q.-J. Zhu and G. Wei, *CrystEngComm*, 2011, **13**, 5105.
20 K. Chen, Y.-F. Hu, X. Xiao, S.-F. Xue, Z. Tao, Y.-Q. Zhang, Q.-J. Zhu and J.-X. Liu, *RSC Adv.*, 2012, **2**, 3217.
21 K. Chen, L.-L. Liang, Y.-Q. Zhang, S.-F. Xue, Z. Tao, Q.-J. Zhu, L. F. Lindoy and G. Wei, *CrystEngComm Submitted.*.
22 Bruker. *SAINT and SADABS*. Bruker AXS Inc., Madison, Wisconsin, USA. 2005.
23 (*a*) *SHELXTL program package*, version 5.1; Bruker AXS, Inc.: Madison, WI; (*b*) G. M. Sheldrick, *Acta Cryst.*, 2008, **A64**, 112.
24 J. X. Liu, L. S. Long, R. B. Huang and L. S. Zheng, *Cryst. Growth Des.*, 2006, **6**, 2611.
25 X. K. Fang, P. Kogerler, L. Isaacs, S. Uchida and N. Mizuno, *J. Am. Chem. Soc.*, 2009, **131**, 432.
26 (*a*) Z. Tao, Q.-J. Zhu, W. G. Jackson, Z.-Y. Zhou and X.-G. Zhou, *Polyhedron*, 2003, **22**, 263; (*b*) R.-G. Lin, Z. Tao, S.-F. Xue, Q.-J. Zhu, W. G. Jackson, Z.-B. Wei and L.-S. Long, *Polyhedron*, 2003, **22**, 3467.
27 F. Zhang, T. Yajima, Y. Z. Li, G. Z. Xu, H. L. Chen, Q. T. Liu and O. Yamauchi, *Angew. Chem., Int. Ed.*, 2005, **44**, 3402.

